Adsorption and Reaction of CO and CO_2 on Oxidized and Reduced $SrTiO_3$(100) Surfaces

Samina Azad and Mark H. Engelhard

Environmental Molecular Science Laboratories, Pacific Northwest National Laboratory, Richland, Washington 99354

Li-Qiong Wang*

Material Science Division, Pacific Northwest National Laboratory, Richland, Washington 99354

Received: September 13, 2004; In Final Form: February 14, 2005

The adsorption and reaction of CO and CO_2 on oxidized and reduced $SrTiO_3$(100) surfaces have been studied with temperature programmed desorption (TPD) and X-ray photoelectron spectroscopy (XPS). XPS results indicate that the oxidized $SrTiO_3$(100) surfaces are nearly defect-free with predominantly Ti^{4+} ions whereas the sputter-reduced surfaces contain substantial amounts of defects. Both CO and CO_2 are found to adsorb weakly on the oxidized $SrTiO_3$(100) surfaces. On sputter-reduced surfaces, enhanced reactivity of CO and CO_2 is observed due to the presence of oxygen vacancy sites, which are responsible for dissociative adsorption of these molecules. Our studies indicate that the CO and CO_2 molecules exhibit relatively weaker interactions with $SrTiO_3$(100) compared to those with TiO_2(110) and TiO_2(100) surfaces. This is most likely an influence of the Sr cations on the electronic structure of the Ti cations in the mixed oxide of $SrTiO_3$.

1. Introduction

Interaction of CO and CO_2 with metal oxide surfaces is an important topic in basic and applied research. Both CO and CO_2 are used as common probe molecules in surface science to obtain fundamental information about the gas−surface interactions, adsorption sites, and reactive dynamics on a variety of metals, semiconductors, and insulator surfaces. Reactions of CO and CO_2 on metal oxides are involved in many technologically important chemical processes at gas−solid and liquid−solid interfaces. CO is one of the most hazardous products released by car exhausts as a result of incomplete combustion whereas CO_2 is a green-house gas. The study of reactions of CO and CO_2 on oxide surfaces is critical to environmental pollution control and development of gas sensors.

Both TiO_2 and $SrTiO_3$ single crystals have been widely used as model surfaces to study the structural and chemical properties of oxide surfaces because of their availability as well as the varieties of oxidation states and coordination environments they provide. Reactivity of these surfaces is largely influenced by the presence of surface defects, acid−base properties of adsorbed molecules and the surface, as well as the geometric arrangement of the surface atoms. Oxygen vacancies or other more complex surface defects, associated with the reduced states of these surfaces, are known to promote the reactions of adsorbed molecules on the metal oxide surfaces. Previous studies revealed that the defect sites on reduced TiO_2(100), TiO_2(110), and $SrTiO_3$(100) surfaces are reoxidized by extraction of the oxygen atoms from the adsorbed molecules on the surface.[1−5]

Reactions of CO and CO_2 have been investigated extensively on TiO_2 surfaces. Similar studies on $SrTiO_3$ surfaces, however, are rare. Various desorption states were observed for adsorption of CO on powdered TiO_2.[6] Conflicting experimental results have been reported for CO adsorption on single-crystal TiO_2 surfaces: Gopel et al.[7] found that oxidation of CO takes place only on a reduced surface whereas Yates and co-workers[8] did not find any evidence of CO oxidation even on defected TiO_2 surfaces. Recently, periodic density functional theory calculations on adsorption of CO and O_2 on stoichiometric and partially reduced TiO_2(110) showed that O_2 adsorption and CO oxidation take place on these surfaces only in the presence of surface oxygen vacancies.[9]

The nature of CO_2 chemisorption on TiO_2 has been reported based on theoretical calculations for adsorption on single crystals.[10] Adsorption of CO_2 has also been studied on both powdered[11−13] and single-crystal surfaces.[14−16] Studies on powdered TiO_2 samples indicated dissociative adsorption of CO_2 on both oxidized and reduced surfaces.[17] TPD studies on reactions of CO_2 on TiO_2(110) surfaces showed weak interactions. Two distinct binding sites were detected on the vacuum annealed surfaces: five-coordinate Ti^{4+} sites and oxygen vacancy sites.[15] CO_2 shows stronger interactions with the defect sites compared to its reactivity on the five-coordinate Ti^{4+} sites of TiO_2(001) and TiO_2(110) surfaces.[18]

This study focuses on the interaction of CO and CO_2 with the TiO_2-terminated oxidized and reduced $SrTiO_3$(100) surfaces. The $SrTiO_3$(100) surface has two possible nonpolar surface terminations: a SrO-terminated surface and a TiO_2-terminated surface. The TiO_2-terminated stoichiometric $SrTiO_3$(100), schematically illustrated in Figure 1, displays a different geometric arrangement for surface Ti and O atoms compared with TiO_2-(110) and TiO_2(100) surfaces. Unlike the rows of two-coordinate bridging oxygen atoms, lying above the rows of Ti atoms in the cases of TiO_2(110) and TiO_2(100) surfaces, the cations on the TiO_2-terminated $SrTiO_3$(100) surface lie essentially on the same plane as the oxygen atoms. In addition to the difference in geometric structures between TiO_2 and TiO_2-terminated $SrTiO_3$ surfaces based on the previous theoretical calculations,[19] Ti−O bonds on the TiO_2-terminated $SrTiO_3$(100) surface are more covalent than those on the TiO_2 surfaces due to the

* To whom correspondence should be addressed. E-mail: lq.wang@pnl.gov.

10.1021/jp045864b CCC: $30.25
Published on Web 04/21/2005

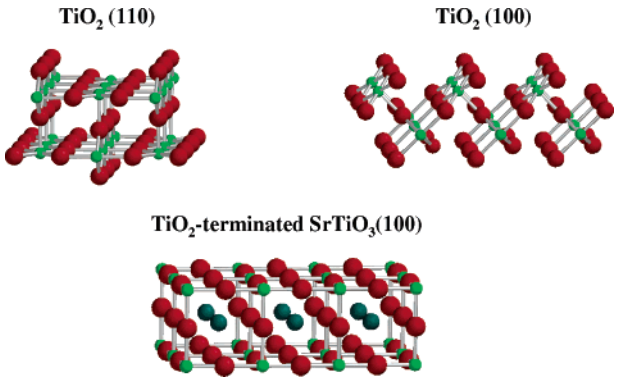

Figure 1. Schematic models for the $TiO_2(110)$, $TiO_2(100)$, and TiO_2-terminated $SrTiO_3(100)$ surfaces.

presence of a large number of Sr atoms in the near-surface region of the $SrTiO_3(100)$ surface.

In this study, we investigate the adsorption and reaction of CO and CO_2 on oxidized and reduced $SrTiO_3(100)$ surfaces using temperature-programmed desorption (TPD) and X-ray photoemission (XPS) techniques. We compare the results obtained from the TiO_2-terminated $SrTiO_3(100)$ surfaces with those from the $TiO_2(110)$ surfaces to obtain a better understanding of the influence of electronic structures, atomic arrangements, and surface defects on the adsorption and reaction of CO and CO_2 on $SrTiO_3(100)$ surfaces.

2. Experimental Section

The $SrTiO_3(100)$ crystals ($10 \times 10 \times 2$ mm^3) were purchased from Princeton Scientific. The crystal used for TPD measurements was epi-polished on both sides and cut with 0.5 mm $\times$ 2.0 mm slots around the four sides of the crystals. The crystal was mounted on a polished tantalum plate with a 0.025 mm thick gold foil sandwiched between the two surfaces. Chromel−alumel thermocouple wires were glued to the sample with a ceramic glue. The sample can be resistively heated to 1000 K, and cooled to 110 K by thermal contact with a liquid-nitrogen-filled reservoir. The samples were cleaned by Ar^+ sputtering and by subsequent vacuum annealing at 850 K. The fully oxidized surfaces were then obtained by annealing at 800−850 K for 10 min, in 1×10^{-7} Torr of O_2, whereas the vacuum-annealed surfaces were obtained by annealing the sample at 800−850 K in a vacuum for 10 min. The sputter-reduced surfaces were prepared by Ar^+ bombardment at 1 kV for 10 min. The samples were dosed via back filling the chamber with the reactant gases. Cleanliness of the samples was verified by AES measurements prior to the TPD and XPS experiments.

TPD studies were performed in an ultrahigh vacuum (UHV) system containing a single pass cylindrical mirror analyzer for Auger electron spectroscopy (AES), a quadrupole mass spectrometer for TPD, optics for low-energy electron diffraction (LEED), and a sputter gun for sample cleaning. During the TPD experiments the desorbing species were detected with a UTI quadrupole mass spectrometer (QMS) interfaced to a PC allowing nine masses to be monitored simultaneously during the desorption sweep. TPD measurements were performed by positioning the crystal in front of the QMS and by using a linear temperature ramp of 4 K/s.

XPS measurements were made in a Physical-Electronics Quantum 2000 scanning ESCA microprobe system with a hemispherical analyzer. Monochromatic Al Kα X-rays (1486.7), with an X-ray spot size of 1.5 mm $\times$ 0.2 mm, were used to generate the spectra. The X-ray beam used was a 101 W, 107

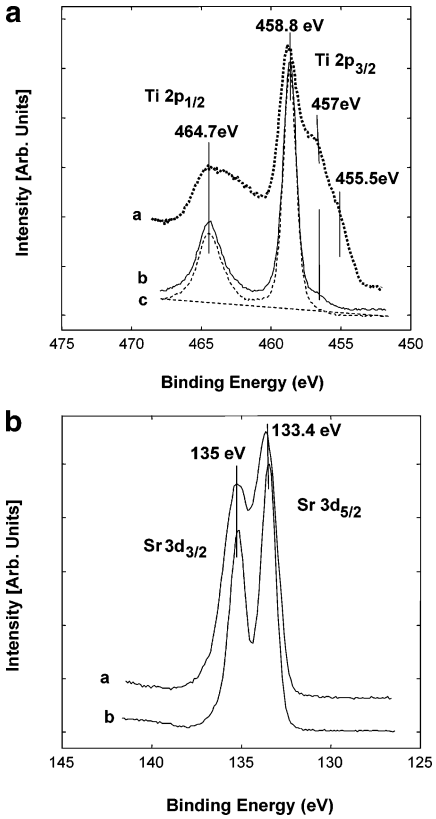

Figure 2. (a) Ti 2p XPS spectra from $SrTiO_3(100)$ surface after (a) sputtering with 1 kV Ar^+, (b) vacuum annealing to 800−850 K, and (c) fully oxidizing in 2×10^{-7} Torr O_2 at 800−850 K. (b) Sr 3d XPS spectra from $SrTiO_3(100)$ surface after (a) sputtering with 1 kV Ar^+ and (b) fully oxidizing in 2×10^{-7} Torr of O_2 at 800−850 K.

μm diameter beam that was rastered over a 1.4 mm $\times$ 0.2 mm rectangle on the sample. The X-ray beam was incident normal to the sample and the photoelectron detector was at 45° off normal. Multiplex data were collected with a pass-energy of 23.5 eV, and were referenced to an energy scale with binding energies for Au 4f at 84 $\pm$ 0.03 eV and Cu $2p_{3/2}$ at 932.67 $\pm$ 0.03 eV. Binding energy positions were referenced with use of a 458.8 eV position for the Ti $2p_{3/2}$ feature.

CO (Matheson, 99.99%) and CO_2 (Matheson, 99.99%) were used as received. The gas exposures in these experiments are given in Langmuir ($1\ \text{L} = 1 \times 10^{-6}$ Torr s). Various exposures of CO and CO_2 were dosed through a leak valve to the crystal at ~110 K, during the TPD studies.

3. Results and Discussion

3.1. XPS Studies on Oxidized, Vacuum Annealed, and Sputter-Reduced $SrTiO_3(100)$. Fully oxidized $SrTiO_3(100)$ surfaces, prepared in our studies by sputtering followed by annealing at 800−850 K in O_2, show a 1×1 LEED pattern. Previous ion scattering studies[20,21] showed that similarly prepared $SrTiO_3(100)$ single crystal surfaces are predominantly terminated by TiO_2 atomic planes. Thus, the stoichiometric or fully oxidized $SrTiO_3(100)$ surfaces used in our studies are predominantly TiO_2 terminated.

We have performed XPS studies to examine the structure and composition of the fully oxidized, vacuum-annealed, and sputter-reduced $SrTiO_3(100)$ in the near-surface regime. Figure 2a displays Ti 2p XPS spectra from Ar^+ sputtered (trace "a"), vacuum-annealed (trace "b"), and fully oxidized (trace "c") $SrTiO_3(100)$. Substantial surface reduction is obtained by Ar^+ sputtering as indicated by the broad Ti $2p_{3/2}$ and Ti $2p_{1/2}$ peaks

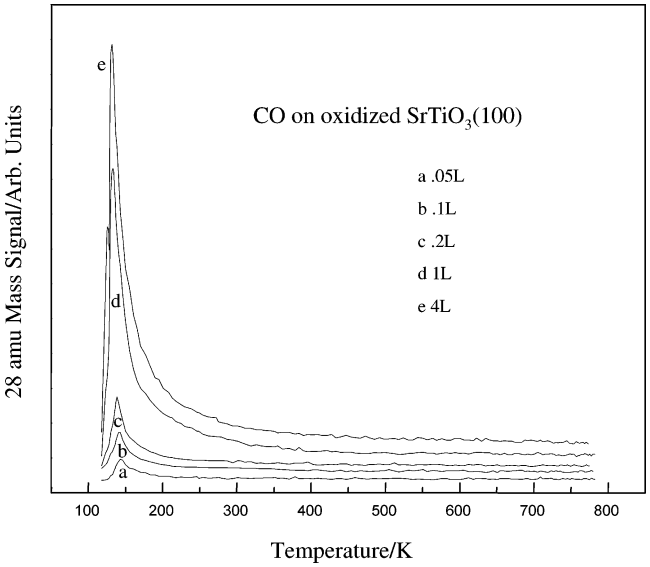

Figure 3. The 28 amu temperature-programmed desorption spectra for CO adsorbed onto an oxidized $SrTiO_3(100)$ surface at 110 K following adsorption of 0.05 (a), 0.1 (b), 0.2 (c), 1 (d), and 4 L (e) of CO.

(trace "a" Figure 2a) that result from the reduced Ti cations (mostly Ti^{3+} and Ti^{2+}) created on the sputtered surface.[22] The spectrum for the fully oxidized surface (trace "c" Figure 2a) contains sharp Ti $2p_{3/2}$ and Ti $2p_{1/2}$ peaks at 458.8 and 464.7 eV, indicating the presence of only Ti^{4+} ions on this surface. The vacuum-annealed surface (trace "b" Figure 2a), prepared by annealing the sputter-reduced surface (presented in trace "a" of the same figure), has the same features as the fully oxidized surface with a small additional peak at 457 eV that is related to the reduced Ti cations. Taking this peak at 457 eV as a measure of the degree of surface reduction, the vacuum-annealed surface was found to contain ~3.5% of reduced Ti cations.[23] These results clearly indicate diffusion of bulk O^{2-} to the surface during annealing, which creates a nearly defect-free surface by reoxidation of the reduced Ti cations. Oxygen diffusion via defect sites is well-known for reduced TiO_2.[24,25] By using the Ti $2P_{3/2}$ peak areas as a measure of the degree of reduction, this heavily reduced sputtered surface prepared in our studies was found to contain ~40% of reduced Ti sites.[23]

The Sr 3d XPS spectra for the fully oxidized (trace "b" of Figure 2b) and sputter-reduced $SrTiO_3(100)$ (trace "a" of Figure 2b) are identical except for the broadening of the 3d peaks due to the surface roughness and disorder created by the sputtering process. These results clearly indicate that Ar^+ sputtering does not reduce the Sr^{4+} cations on the $SrTiO_3(100)$ surfaces. The XPS results observed in this study are consistent with the surface studies on the oxidized and reduced $SrTiO_3$ surfaces that we have published previously.[3,19,26,27]

3.2. CO on Oxidized and Reduced $SrTiO_3(100)$. The TPD features for CO on the vacuum-annealed surface are identical with those obtained from the fully oxidized $SrTiO_3(100)$, indicating that vacuum annealing creates very little defect sites, and these results are in good agreement with our XPS results. In describing the TPD results, the 'fully oxidized surface" and the "vacuum-annealed surface" will both be referred to as the "oxidized surface". Figure 3 displays a series of 28 amu TPD spectra following adsorption of 0.05 (a), 0.1(b), 0.2 (c), 1 (d), and 4 L (e) of CO at 110 K on the oxidized $SrTiO_3(100)$ surface. At low coverage, the CO spectrum consists of a feature at ~140 K, which shifts slightly toward lower temperature with increasing coverage, and is assigned to desorption of weakly bound

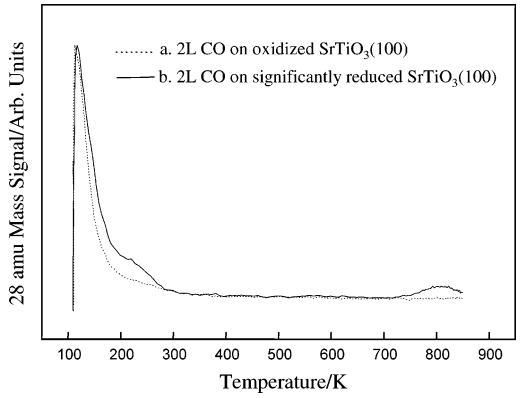

Figure 4. The 28 amu temperature-programmed desorption spectra following adsorption of 2 L of CO on oxidized (a) and significantly reduced (b) $SrTiO_3$ surfaces at 110 K.

CO on this surface. The shift to a lower binding energy with increasing coverage can be attributed to repulsive dipole−dipole interactions of the adsorbed CO molecules. The desorption feature for CO is asymmetric, with a tail on the higher temperature side. The absence of higher temperature desorption states in the CO TPD spectra obtained in our studies suggests that CO does not dissociate on the oxidized $SrTiO_3(100)$ surface**.**

Figure 4 compares TPD spectra for CO (28 amu) following adsorption of 2 L of CO from oxidized (part a) and sputter-reduced (part b) $SrTiO_3(100)$ at 110 K. Three TPD features, at 140, 220, and 812 K, are observed for desorption of CO from the sputter-reduced surface. As observed in Figure 4b, the majority of the CO molecules desorbs around 140 K, in a peak resulting from the molecular desorption of weakly adsorbed CO from the heavily reduced $SrTiO_3(100)$ following adsorption at 110 K. The feature at 220 K indicates a second desorption state with a higher desorption energy and most likely results from interaction of the adsorbed CO molecules with oxygen vacancy sites. As reported in a previous study,[28] the presence of O-vacancy sites strongly enhances the CO interaction with the surface due to a large electron back-donation from reduced cations such as Ti^{3+} ions on the surface to the adsorbed CO molecules. Partial dissociation of the CO molecules on the sputter-reduced surface is indicated by desorption of CO from this sputter-reduced surface above 800 K. Formation of adsorbed C and O atoms and recombination of these species at higher temperature to desorb as molecular CO is suggested by the 812 K feature from the reduced surface (Figure 4b). A second set of TPD experiments following the initial set from the significantly reduced surface produce similar results as those obtained from the oxidized surface indicating that the sputter-induced damage of this surface is mostly healed and the reduced surface is reoxidized during the annealing process. A negligible amount of CO_2 is observed during TPD from both oxidized and reduced $SrTiO_3(100)$ surfaces following exposure to CO, indicating almost no oxidation of CO on $SrTiO_3(100)$ surfaces, in agreement with the previous study of CO on $TiO_2(110)$ surfaces.[8] At similar low coverages, CO desorbs from the oxidized $SrTiO_3(100)$ at slightly lower temperature (~140 K) compared to that from the oxidized $TiO_2(110)$ surface (~170 K) where 43 kJ mol^{-1} is the estimated desorption energy for CO from the latter surface.[8] Previous theoretical calculations[29] also indicated larger desorption energy (46 kJ mol^{-1}) for CO on $TiO_2(110)$ compared to that on $SrTiO_3(100)$.

Identical TPD spectra are obtained from $SrTiO_3(100)$ surfaces prepared by a series of vacuum annealing cycles. As observed in our XPS and TPD studies, annealing the sputter-reduced

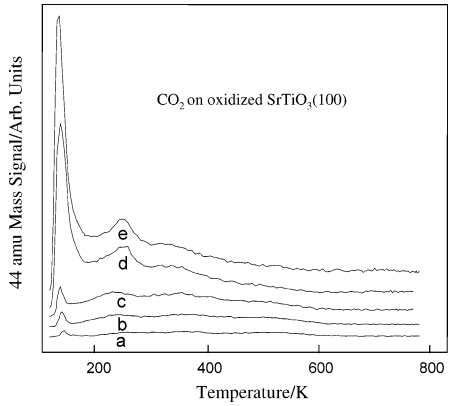

Figure 5. The 44 amu temperature-programmed desorption spectra for CO_2 adsorbed onto an oxidized $SrTiO_3(100)$ surface at 110 K following the adsorption of 0.02 (a), 0.05 (b), 0.1 (c), 0.3 (d), and 0.5 L (e) of CO_2.

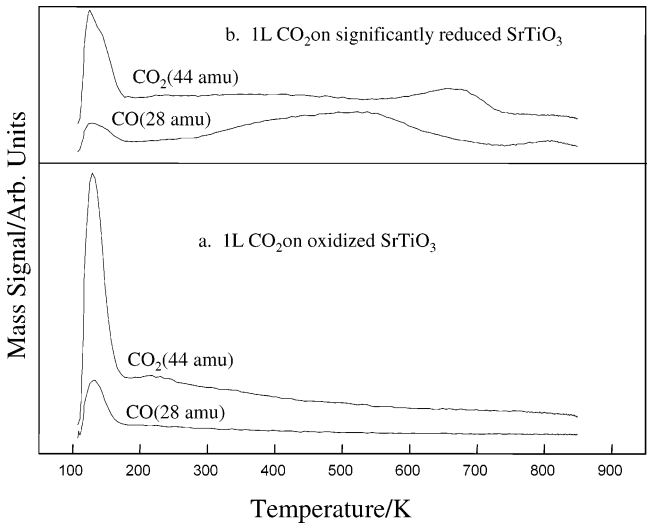

Figure 6. Temperature-programmed desorption spectra following adsorption of 1 L of CO_2 at 100 K on oxidized (a) and significantly reduced (b) $SrTiO_3$ surfaces.

surface at 850 K removes the sputter-induced damages and reoxidizes the reduced surface to a nearly defect-free surface. These results are in good agreement with our previous studies on $SrTiO_3(100)$ surfaces.[3,26,27] On $TiO_2(110)$ surfaces, however, a significant amount of oxygen vacancy sites were created by using controlled annealing conditions where an increase in the desorption temperature of a portion of the CO chemisorbed on the annealed surface was observed.[8] As mentioned earlier, dissociation or thermal oxidation of CO was not observed on the thermally annealed $TiO_2(110)$ surfaces in the studies of Yates et al. whereas oxidation of CO on reduced $TiO_2(110)$ has been reported by Gopel et al. and Wu et al.[7,9]

3.3. CO_2 on Oxidized and Reduced $SrTiO_3(100)$. Figure 5 displays a series of 44 amu TPD spectra for CO_2 adsorbed on oxidized $SrTiO_3(100)$ surface following adsorption of 0.02 (a), 0.05 (b), 0.1 (c), 0.3 (d), and 0.5 L (e) of CO_2 on this surface. The 44 amu TPD spectrum for 1 L of CO_2 exposure on the oxidized $SrTiO_3(100)$ surface is given in Figure 6a. Weak interaction of CO_2 with the oxidized surface is apparent from the sharp peak at ~132 K. This 132 K feature grows in intensity with increasing exposure and the majority of CO_2 desorbs molecularly at 132 K from the oxidized surface. Weak higher temperature features shown in Figure 6a may result from adsorption of CO_2 on a small amount of defect sites that may be present on the oxidized surface.

These results agree well with similar work done on oxidized $TiO_2(110)$ surfaces; however, the interaction of CO_2 on the oxidized $SrTiO_3(100)$ surface is weaker than that on stoichiometric $TiO_2(110)$ as indicated by the higher desorption temperature of CO_2 (170 K) on the latter surface at similar low coverages.[18] Previous studies on the interaction of CO_2 on TiO_2-(110) surfaces revealed that vacuum annealing creates substantial amounts of oxygen vacancies on this surface[15,18] whereas the vacuum-annealed $SrTiO_3(100)$ surfaces contain very few defect sites as indicated by our XPS and TPD results.

The corresponding TPD spectra monitoring desorption of CO (28 amu) and CO_2 (44 amu) are displayed for a 1 L of CO_2 exposure at 110 K to the oxidized (Figure 6a) and sputter-reduced (Figure 6b) $SrTiO_3(100)$. As observed in Figure 6b, the desorption state at ~130 K results from desorption of weakly adsorbed CO_2 from the reduced $SrTiO_3(100)$ whereas the 650 K desorption feature is presumably due to interaction of CO_2 with the oxygen vacancy sites on this surface. In the 28 amu spectrum in the same figure (Figure 6b), a broad desorption state centered at ~500 K and a very weak feature at 800 K are observed for desorption of CO from this surface. The broad feature of CO (350−650 K) most likely results from the preferential extraction of O atoms of the adsorbed CO_2 by the oxygen vacancy sites on the reduced $SrTiO_3(100)$ surfaces. The weak CO feature at above 800 K (Figure 6b) suggests partial dissociation of CO_2 on the reduced surface to produce adsorbed C and O atoms that recombine to form CO during the TPD process. As observed for reactions of CO on this surface, a second set of TPD experiments following the initial set from the sputter-reduced surface produce similar results as found on the oxidized surface indicating reoxidation of the reduced surface during thermal annealing. Previous studies[15,18] reported similar results for reduced $TiO_2(110)$ surfaces, suggesting that CO_2 molecules are reduced on these surfaces along with a corresponding reoxidation of the substrate surfaces. The $TiO_2(110)$ surfaces, however, are reduced to a much higher extent by vacuum annealing compared to the $SrTiO_3(100)$ surfaces. Systematic production of increasing levels of surface defects, on the $TiO_2(110)$, is observed in the annealing temperature range of 600−1100 K.[18]

3.4. Reactivity of TiO_2-Terminated $SrTiO_3(100)$ and TiO_2-(110). As observed in our study, the desorption temperatures for both CO and CO_2 are lower on the TiO_2-terminated $SrTiO_3$-(100) surface compared to those on $TiO_2(110)$ and $TiO_2(100)$ surfaces. This difference in desorption temperature may be attributed to the difference in both geometric and electronic structures of these surfaces. Our previous studies revealed that water exhibits relatively stronger interactions with the TiO_2-(110) and $TiO_2(100)$ surfaces than with the $SrTiO_3(100)$ surface.[30] The nature of the Ti^{4+} cation sites was found to be more covalent on the TiO_2-terminated $SrTiO_3(100)$ compared to the same sites on the TiO_2 surfaces based on electronic structural calculations,[19,31] and these differences can be attributed primarily to the influence of the Sr cations on the electronic structure of the Ti cations in the mixed oxide of $SrTiO_3$. In particular, as was proposed in previous calculations on the energetics of mixed metal oxide surfaces, in the mixing of two oxides (one having a more ionic cation than the other), the ionic properties of the more ionic cation are expected to increase further, while the covalent properties of the more covalent ion should also be enhanced.[19] Thus the higher covalence or weaker acidity of Ti^{4+} cations on $SrTiO_3(100)$ surfaces results in a weaker acid−base interaction between Ti^{4+} sites and water. In the case of the reactions of water on this surface, the absence

of the bridging oxygen atoms on the $SrTiO_3(100)$ surface (Figure 1), that serve to aid the binding of water via hydrogen bonding,[32] may also be responsible for the weaker adsorption of H_2O on $SrTiO_3(100)$. Since CO and CO_2 do not have hydrogen bonding interactions with the surface, the lower covalence of Ti^{4+} cations on the $SrTiO_3(100)$ surface attributes predominantly to a weaker interaction of CO and CO_2 with this surface compared to similar interactions on the $TiO_2(110)$ and (1×1) $TiO_2(100)$ surfaces.

Based on the TPD and XPS results performed in our studies, vacuum annealing does not create a substantial amount of defects on $SrTiO_3(100)$ suggesting that the reducibility of these surfaces is significantly lower compared to that of the TiO_2-(110) surfaces which get reduced extensively as a result of vacuum annealing, in agreement with our previous study.[26] Migration of O^{2-} from the bulk to the surface during thermal annealing reoxidizes the former surface. The differences in geometric structures between TiO_2-terminated $SrTiO_3(100)$ and $TiO_2(110)$ and $TiO_2(100)$ surfaces may also be partially responsible for the different patterns in dissociation of CO and CO_2 on these surfaces. Dissociative adsorption of CO and CO_2 was not observed on vacuum-annealed $SrTiO_3(100)$ surfaces whereas CO_2 is found to adsorb dissociatively on vacuum-annealed $TiO_2(110)$ surfaces.

4. Conclusions

Adsorption and reaction of CO and CO_2 have been studied on oxidized and reduced $SrTiO_3(100)$ surfaces. XPS studies have been performed to estimate the amount of surface reduction produced by vacuum annealing and sputter reduction. These results indicate that the fully oxidized and vacuum-annealed $SrTiO_3(100)$ surfaces are nearly defect-free with predominantly Ti^{4+} ions whereas the sputter-reduced surface contains substantial amount of defects (~40% reduced Ti sites). Desorption of CO is observed at 140 K from the oxidized $SrTiO_3(100)$ following adsorption at ~110 K. A higher temperature desorption feature is also observed in the CO TPD spectrum from the highly reduced surface and this is presumably due to interaction of CO with the oxygen vacancy sites. Dissociation of CO on the sputter-reduced $SrTiO_3(100)$ and recombination of the adsorbed C and O atoms during the TPD process is indicated by desorption of CO from this surface at temperatures above 800 K. Most of the adsorbed CO_2 desorbs around 132 K from the oxidized surfaces. Dissociation of CO_2 on sputter-reduced $SrTiO_3(100)$ is apparent by the presence of high-temperature desorption states for CO_2 in the TPD spectra. TPD and XPS results indicate that high-temperature vacuum annealing (800−850 K) does not create substantial amounts of surface defects and that the reactivity of the annealed surface is similar to that of the fully oxidized surface. These results also indicate reoxidation of the sputter-reduced $SrTiO_3(100)$ during thermal annealing. CO and CO_2 exhibit weaker interactions with $SrTiO_3$-(100) compared to those with the $TiO_2(110)$ and $TiO_2(100)$ surfaces. Influence of the Sr cations on the electronic structure of the Ti cations in $SrTiO_3$ is most likely responsible for this enhanced reactivity.

Acknowledgment. This work was supported by the Division of Materials Sciences, Office of Basic Energy Sciences, U.S. Department of Energy (USDOE). The experiments were performed in the Environmental Molecular Science Laboratories (EMSL), a national scientific user facility located at Pacific Northwest National Laboratory (PNNL) and supported by the U.S. Department of Energy's Office of Biological and Environmental Research. PNNL is a multiprogram national laboratory operated for the USDOE by Battelle Memorial Institute under Conduct No. DE-AC06-76RLO.

References and Notes

(1) Wang, L.-Q.; Ferris, K. F.; Skiba, P. X.; Shultz, A. N.; Baer, D. R.; Engelhard, M. H. *Surf. Sci*. **1999**, *440*, 60.
(2) Azad, S.; Wang, L.-Q.; Szanyi, J.; Peden, C. H. F. *J. Vac. Sci. Technol. A* **2003**, *21*, 1307.
(3) Wang, L.-Q.; Ferris, K. F.; Winokur, J. P.; Shultz, A. N.; Baer, D. R.; Engelhard, M. H. *J. Vac. Sci. Technol. A* **1998**, *16*, 3034.
(4) Wang, L.-Q.; Schultz, A. N.; Baer, D. R.; Engelhard, M. H. *J. Vac. Sci. Technol. A* **1996**, *14*, 1532.
(5) Wang, L.-Q.; Baer, D. R.; Engelhard, M. H. *Surf. Sci.* **1995**, *344*, 237.
(6) (a) Beck, B. B.; White, J. M.; Ratcliffe, C. T. *J. Phys. Chem.* **1986**, *90*, 3132. (b) Boccuzzi, F.; Chiorino, A.; Manzoli, M. *Surf. Sci.* **2002**, *502*, 513.
(7) Gopel, W.; Rocker, G.; Freierabend, R. *Phys. Rev. B* **1983**, *28*, 3427.
(8) Linsebigler, A.; Lu, G.; Yates, J. T., Jr. *J. Chem. Phys.* **1995**, *103*, 9438.
(9) Wu, X.; Selloni, A.; Nayak, S. *J. Chem. Phys.* **2004**, *120*, 4512.
(10) Markovits, A.; Fahmi, A.; Minot, C. *THEOCHEM* **1996**, *371*, 219.
(11) Tanaka, K.; White, J. M. *J. Phys. Chem.* **1982**, *86*, 3977.
(12) Tanaka, K.; Miyahara, K.; Toyoshima, I. *J. Phys. Chem.* **1984**, *88*, 3504.
(13) Yanagisawa, Y.; Sumitomo, T. *Appl. Phys. Lett.* **1994**, *64*, 3343.
(14) Gopel, W.; Rocker, G.; Freierabend, R. *Phys. Rev. B* **1983**, *28*, 3427.
(15) Henderson, M. A. *Surf. Sci.* **1998**, *400*, 203.
(16) Wilson, J. N.; Senanayake, S. D.; Idriss, H. *Surf. Sci.* **2004**, *562*, L231.
(17) Raupp, G. B.; Dumesic, J. A. *J. Phys. Chem.* **1985**, *89*, 5240.
(18) Thompson, T.; Diwald, O.; Yates, J. T., Jr. *J. Phys. Chem. B* **2003**, *107*, 11700.
(19) Rodriguez, J. A.; Azad, S.; Wang, L.-Q.; Garcia, J.; Etxeberria, A.; Gonzalez, L. *J. Chem. Phys.* **2003**, *118*, 6562.
(20) Yoshimoto, M.; Maeda, T.; Shimozono, K.; Koinuma, H.; Shinohara, M.; Ishiyama, O.; Ohtani, F. *Appl. Phys. Lett.* **1994**, *65*, 3197.
(21) Nishimura, T.; Ikeda, A.; Namba, H.; Morishita, T.; Kida, Y. *Surf. Sci.* **1999**, *421*, 273.
(22) Szabo, A.; Engel, R. *Surf. Sci.* **1995**, *329*, 241.
(23) Mayer, J. T.; Diebold, U.; Madey, T. E.; Garfunkel, E. *J. Electron Spectrosc. Relat. Phenom.* **1995**, *73*, 1.
(24) Drobeck, D. L.; Vikar, A. V.; Cohen, R. M. *J. Phys. Chem. Solids* **1990**, *51*, 977.
(25) Dennis, P. F.; Freer, R. *J. Mater. Sci.* **1993**, *28*, 4804.
(26) Wang, L.-Q.; Ferris, K. F.; Herman, G. S.; Engelhard, M. H. *J. Vac. Sci. Technol. A* **2000**, *18*, 1893.
(27) Wang, L.-Q.; Ferris, K. F.; Shultz A. N.; Baer, D. R.; Engelhard, M. H. *Surf. Sci.* **1997**, *380*, 352.
(28) Sorescu, D. C.; Yates, J. T., Jr. *J. Phys. Chem. B* **2002**, *106*, 6184.
(29) Sorescu, D. C.; Yates, J. T., Jr. *J. Phys. Chem. B* **1998**, *102*, 4556.
(30) Wang, L.-Q.; Ferris, K. F.; Herman, G. S. *J. Vac. Sci. Technol. A* **2002**, *20*, 239.
(31) Barr, T. L. *J. Vac. Sci. Technol. A* **1991**, *9*, 1793.
(32) Ferris, K. F.; Wang, L.-Q. *J. Vac. Sci. Technol. A* **1998**, *16*, 956.